

# Passive Position Controlled Telepresence Systems with Time Delay

Sandra Hirche     Martin Buss

Control Systems Group  
Faculty of Electrical Engineering and Computer Science  
Technical University of Berlin, Germany  
hirche@rs.tu-berlin.de     M.Buss@ieee.org

## Abstract

This paper discusses combined position and force control of telepresence systems with force feedback and time delay. Standard architectures use velocity/force control and well known passivity arguments. Disadvantageously, then the positions of the Human System Interface (HSI) and the teleoperator diverge in presence of disturbances, deteriorating transparency. In this paper a new method for impedance matching filter design by optimization in the frequency domain to achieve passivity of the teleoperator/environment and transparency of position-force controlled telepresence systems is proposed. The validity of the approach is shown in simulations and experimental results.

## 1 Introduction

Bilateral telemanipulation systems with force (also called kinesthetic or haptic) feedback allow a human operator to be active in a distant, possibly hazardous environment. Telepresence is a key technology for many applications, e.g. telesurgery, teleservice, telemanufacturing, teleshopping. Telepresence systems are now mostly implemented in communication infrastructures like the Internet with substantial (varying) time delay of several hundred milliseconds. Without control measures time delay impairs kinesthetic transparency (the feeling of direct interaction with remote environment) or may even cause instability.

This paper is focused on bilateral telemanipulation with *constant* time delay, for a discussion of the varying delay problem see the companion paper [1]. The here proposed method is based on known passivity arguments. Main contribution is that the position controlled subsystem of teleoperator together with the environment are made passive by impedance matching filters, which are designed by an optimization method in the frequency domain. The advantage of position control is that disturbances do not cause a position deviation of the HSI and the teleoperator. Optimization is required to obtain passive impedance matching filters. One disadvantage of the presented approach is the required environment model knowledge; note that the proposed method is quite robust against model uncertainties.

An overview of related work can be found in [2, 3]. Telepresence systems are usually modeled by a network  $n$ -port approach with forces as effort, velocity as flow, and impedances. Our approach uses position and generalized impedances. Passivation of telepresence systems has been proposed in [4, 5]. Here, the passivation of the communication network two-port is equivalent to these approaches. One novel idea in this paper is that the position controlled teleoperator together with the environment are made robustly passive by appropriately designed impedance matching filters. These have been first proposed in [6], however, the design was heuristic without guaranteeing robust passivity. Our approach has the additional benefit that transparency is improved; see [2, 3, 7–9] for a discussion about other methods like e.g. the four-channel architecture to achieve transparency.

For the organization of the paper: in Section 2 the fundamental concepts of passivity, the telepresence system architecture, impedance matching, and transparency are discussed. The optimization method for the impedance matching filters is proposed in Section 3. Sections 4 and 5 present numerical, simulation, and experimental results.

## 2 Background

A telepresence system with force feedback basically consists of the human system interface (HSI) with a human manipulating it and an executing robot (teleoperator) interacting with a remote environment, ideally tracking the position of the HSI while the human 'feels' the environmental force. The basic structure in network representation is shown in Fig. 1. Based on stability arguments in standard architectures the HSI velocity is communicated to the remote site. In our approach the HSI *position* is transmitted, used as reference  $x_t^d$  for the position controlled teleoperator. The environmental force  $f_e$  measured at the remote site is reflected to the operator, used as reference signal  $f_h^d$  for the force control of the HSI. The input/output behavior of the environment and the mechanical subsystems HSI, teleoperator can be described by their mechanical impedance, the ratio



appropriately chosen controller parameters of the local velocity/force control loops. A trade-off between control loop performance and impedance matching is usually necessary, theoretically ideal matching over all frequencies is generally not possible.

The main drawback of a velocity-force architecture is the non-recoverable position deviation after a disturbance, which can be critical depending on the application area. The communication of position information instead of velocities improves this. The position-force architecture though is not necessarily passive. In [6] a position-force control architecture for telepresence systems using appropriately designed impedance matching filters  $N_x$ ,  $N_0$ , see Fig. 1, is suggested. These filters passify the teleoperator/environment subsystem and aim at matching the impedance over a broader range of frequencies, hence improve transparency. In [6] the filter was designed heuristically, in the following a filter design method using optimization is proposed.

### 2.3 Position-Force Architecture

With the design rule for the impedance matching filters  $N_x$ ,  $N_0$  according to [6]

$$N_x(s) = \frac{1}{\sqrt{Z_2(s)}}, \quad N_0(s) = \frac{1}{N_x(s)} \quad (5)$$

the terminating impedance  $Z_x$ , describing the input/output behavior of the position controlled teleoperator in interaction with a continuous environment and the filters  $N_x$

$$Z_x(s) = \frac{f_e^*(s)}{x_t^{d*}(s)} = N_x^2(s) Z_2(s) = 1$$

matches the characteristic impedance of the communication line  $Z_{comm} = 1$ .

Assuming the terminating impedance to be a stable minimum phase structure it is robustly passive with  $\alpha = \gamma = 0.5$ , see (2) and (3). The passivity and stability argument of the position-force architecture is that the position controlled teleoperator together with the environment, forming  $Z_2(s)$ , is robustly passified by appropriate choice of the impedance matching filter  $N_x$ . Then, the combination with the communication network with arbitrary, constant time delay remains also passive, i.e.  $Z_0(s)$  is passive. Referring again to Fig. 1, the transmitted impedance may be rewritten as

$$Z_1(s) = N_0^2(s) \frac{1 + A e^{-s(T_1+T_2)}}{1 - A e^{-s(T_1+T_2)}}, \quad A = \frac{Z_x(s) - 1}{Z_x(s) + 1}.$$

Applying (5), the filters  $N_0$  recover the impedance  $Z_2$  so that  $Z_1(s) = Z_2(s)$ . Assuming an ideal HSI,  $Z^* = Z_1$ , and an ideal teleoperator,  $Z_2 = Z_e$ , the transparency condition (4) is met, the human operator can feel the environment impedance.

The impedance  $Z_1$  is not necessarily passive because of the possible non-passivity of the teleoperator/environment  $Z_2$ ,

however, if desirable a position controller could be designed in such a way that  $Z_2$  is passive. A decision whether this is beneficial or not mainly has to be based on human factors, which is the reason why this discussion is deferred to a future paper including psycho-physical task performance evaluation aspects.

In practice the ideal filters  $N_x$ ,  $N_0$  are not available as it requires the computation of the square root of an arbitrary transfer function according to (5), which can only be approximated. A novel approach to obtain this approximation by optimization is discussed in the following.

## 3 Filter Optimization by Loop Shaping

Goal of optimization is to design the filter  $N_x$  such that  $Z_x$  approximates the desired terminating impedance  $Z_x^d = 1$  in order to provide a robustly passive filter/teleoperator/environment  $Z_x$  subsystem, see Fig. 2.

### 3.1 Filter Parametrization

The application of passivity condition (1) in the frequency domain requires a stable minimum phase structure  $Z_x$ . This implies that the teleoperator/environment impedance  $Z_2$  as well as the filter transfer function are stable minimum phase structures. Consequently the filter  $N_x$ , considered as a lead-lag filter with

$$N_x(s) = q_1 \frac{s + q_2}{s + q_3} \prod_{i=1}^N \frac{s^2 + q_{4i}s + q_{4i+1}}{s^2 + q_{4i+2}s + q_{4i+3}}$$

is required to have its real and complex poles/zeros in the left half of the complex plane. The optimization parameter vector  $\mathbf{q}$  then must be positive real,  $\mathbf{q} \in \mathbb{R}_+^{4N+3}$ . The Optimization minimizes the following proposed filter design objective function.

### 3.2 Objective Function

The objective function is defined in the complex plane based on the Nyquist plot of the terminating impedance  $Z_x(j\omega, \mathbf{q})$ , see Fig. 2. The main goal of optimization is incorporated in the impedance matching objective.

**Impedance Matching Objective:** The distance  $r_t(j\omega, \mathbf{q}) = |Z_x(j\omega, \mathbf{q}) - Z_x^d|$  between the current terminating and the desired impedance, see Fig. 2, represents a measure of approximation quality. In order to enforce the optimizer to find a robustly passive optimal solution with its Nyquist plot within a small disk around  $Z_x^d = 1$ , see (2) and (3), the integral of squared distances  $r_t^2(j\omega, \mathbf{q})$  is considered to define the impedance matching objective

$$f_t(\mathbf{q}) = \int_0^\infty \alpha_t(\omega) r_t^2(j\omega, \mathbf{q}) d\omega, \quad (6)$$

with the frequency dependent weighting filter  $\alpha_t(\omega)$ . The closer the Nyquist plot of a solution is to  $Z_x^d = 1$ , the less it

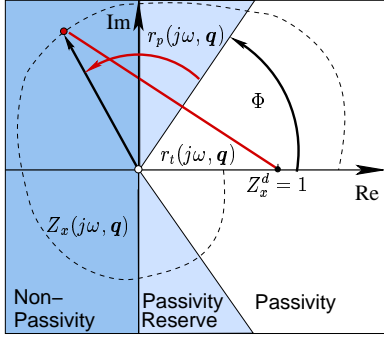


**Figure 2:** Filter optimization by loopshaping of the terminating impedance  $Z_x(j\omega, \mathbf{q})$  in the Nyquist plot.

is penalized. If a solution  $Z_x(j\omega, \mathbf{q})$  is equal to  $Z_x^d = 1$ , the impedance matching objective computes to zero.

During optimization all candidate solutions yielding a non-passive terminating impedance  $Z_x$ , i.e. with the Nyquist plot leaving the right half plane, must be excluded. Implementing this demand in an inequality constraint  $|\angle Z_x(j\omega, \mathbf{q})| < 90^\circ$  according to (1) or in a switching penalty term, resulting in a non-continuous objective function, usually deteriorates the convergence of gradient based optimizers. An additional passivity smooth penalty term enforcing passive solutions together with the impedance matching objective is incorporated in the objective function.

**Passivity Penalty Term:** The passivity objective penalizes any solution for which the terminating impedance  $Z_x(j\omega, \mathbf{q})$  does not stay within the sector  $[-\Phi, +\Phi]$ , represented by the white area in Fig. 2. The angle  $r_p(j\omega, \mathbf{q}) = |\angle Z_x(j\omega, \mathbf{q})| - \Phi$  defines the angular distance between the phase of the terminating impedance  $Z_x(j\omega, \mathbf{q})$  and the sector of passivity. The integral of the squared angles  $r_p^2(j\omega, \mathbf{q})$  over all frequencies  $\omega$  is the passivity penalty term as

$$f_p(\mathbf{q}) = \begin{cases} 0 & \text{for } |\angle Z_x(j\omega, \mathbf{q})| < \Phi \\ \int_0^\infty \alpha_p(\omega) r_p^2(j\omega, \mathbf{q}) d\omega & \text{otherwise,} \end{cases} \quad (7)$$

with  $\alpha_p(\omega)$  weighing the frequency bands of interest. Solutions with the Nyquist plot remaining within the sector  $[-\Phi, +\Phi]$  are not penalized, high phase difference  $r_p(j\omega, \mathbf{q})$  results in high penalty.

**Objective Function** Adding the passivity and transparency objective with relative weight  $\beta > 0$  yields the objective function

$$f(\mathbf{q}) = f_t(\mathbf{q}) + \beta f_p(\mathbf{q}). \quad (8)$$

The convergence of optimization depends on the weights  $\beta$ ,  $\alpha_p(\omega)$ ,  $\alpha_t(\omega)$ , due to its problem dependency the appropriate choice is left to the designer. In theory the impedance matching objective only is sufficient as it targets not only

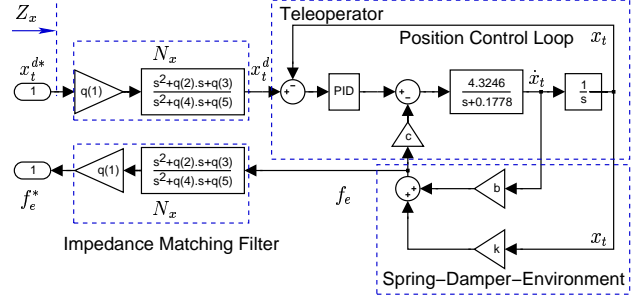


**Figure 3:** SIMULINK blockset of teleoperator, environment and filter for optimization.

transparency, but also robust passivity, as shown in Section 2. Optimization though should generate passive solutions exclusively, hence by adding the passivity penalty term the optimizer is forced to leave the parameter space of non-passive solutions.

## 4 Numerical and Simulation Results

### 4.1 Model Parameters

The filter parameter optimization is performed in the MATLAB/SIMULINK environment. The SIMULINK model shown in Fig. 3 represents the terminating impedance  $Z_x$ , containing the model of a position controlled single-degree-of-freedom (1 DOF) teleoperator, used in experiments with environment and the filter  $N_x$  with parameter vector  $\mathbf{q}$  to be optimized. The nominal environment is defined by a bidirectional stiffness (spring), proportional to the position deviation  $x_t$  from zero with the stiffness coefficient  $k = 1$ . The damping coefficient is set to  $b = 0$ , transmission factor  $c = 1$ . The position control is performed by the PD-controller

$$G_c(s) = P + D \frac{s}{N s + 1}$$

with the parameters  $P = 70$ ,  $D = 10$  and  $N = 100$ . The bode plot of  $Z_2(s)$  in Fig. 4, shows that the mapping between the desired position  $x_t^d$  and the environmental force  $f_e$  is *not passive* because the phase between the signals exceeds  $-90^\circ$ , thus violates the passivity condition (1). After connecting the teleoperator with the passivated transmission line with the time delays  $T_1 = T_2 = 0.2s$  in forward and backward paths the bode plot of the transmitted impedance  $Z_1(j\omega)$  in Fig. 4 exceeds  $-180^\circ$  at magnitudes higher than 0dB, hence is unstable.

### 4.2 Optimization Parameters

For evaluation of the objective function (8) the integrals (7) and (6) are numerically solved by Euler integration in the frequency interval  $[10^{-3}, 10^3]$  rad/s. The values of the filter functions  $\alpha_p(\omega)$  and  $\alpha_t(\omega)$  are specified heuristically and set according to Table 1. The objective function (8) with the weight  $\beta = 1000$  is minimized by the `fminsearch` algorithm of MATLAB.

**Table 1:** Value of filter functions  $\alpha_p(\omega), \alpha_t(\omega)$

Frequency band [rad/s]	$\alpha_p(\omega), \alpha_t(\omega)$
$[10^{-3}, 10^{-2})$	1000
$[10^{-2}, 10^0)$	200
$[10^0, 10^2)$	100
$[10^2, 10^3]$	1

### 4.3 Optimum for Nominal Environment

Higher filter order generally results in better approximation with increased computational cost. In the following a second order lead-lag filter with the optimal parameter vector

$$\mathbf{q}^* = [q_1 \quad q_2 \quad q_3 \quad q_4 \quad q_5] \\ = [3.0 \cdot 10^6 \quad 9.5 \cdot 10^1 \quad 3.2 \cdot 10^3 \quad 2.1 \cdot 10^8 \quad 9.8 \cdot 10^9]$$

resulting in the objective function value of  $f(\mathbf{q}^*) = 6.32$  is used. As a result the terminating impedance  $Z_x(\mathbf{q}^*)$  with the optimal filters  $N_x(\mathbf{q}^*)$  defines a passive mapping as illustrated in the Bode plot in Fig. 6. The closer its magnitude is to the 0dB-line and its phase to the  $0^\circ$ -line, the better the impedances of transmission line and modified teleoperator/environment subsystem match. The small deviation between the bode plots of the transmitted impedance  $Z_1$  and the teleoperator/environment impedance  $Z_2$  as illustrated in Fig. 4 verifies that a high level of transparency in terms of the definition (4) is achieved. Also the tracking behav-

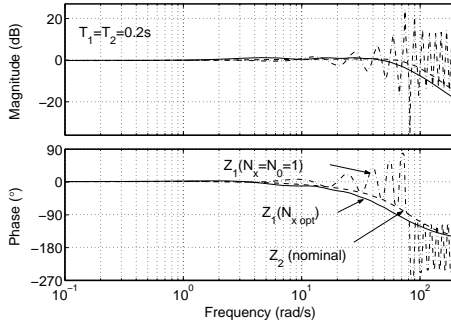


**Figure 4:** Bode plots of teleoperator/environment (dashed), transmitted impedance without filters (dash-dotted) and with optimized filters (solid).

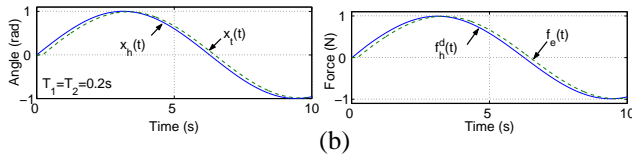


**Figure 5:** Time responses of position and force in nominal environment ( $k = 1$ ) with optimized filters.

ior shown by the time responses of position  $x_t(t)$  and force  $f_e(t)$ ,  $f_h^d(t)$  at teleoperator and the HSI, respectively, to a position input  $x_h(t)$  at the HSI in Fig. 5 is good. Due to the

feedback paths at the HSI side with the filters  $N_0$  containing the model of the environment, the force feedback is not delayed with respect to the position change at the HSI. The human operator has a transparent impression over a broad range of frequencies.

### 4.4 Robustness

The optimized filters  $N_x$  and  $N_0$  contain the model of the environmental impedance, hence system performance is optimal only for the nominal environment, here  $k = 1$ . Small changes in environmental parameters though should not destabilize the system. In the following simulations the influence of the environmental stiffness  $k = 10$  and  $k = 100$  on the terminating impedance  $Z_x$  is exemplarily investigated, illustrated in the bode plots in Fig. 6. The  $\pm 90^\circ$ -line is not crossed, thus even for such large parameter uncertainties the system remains passive. The teleoperator position responses  $x_t(t)$  to a sinusoidal position signal  $x_h(t)$  at the HSI show a decrease in tracking performance for deviating environmental stiffness, see Fig. 7. The impact of model uncertainty on the tracking performance decreases for lower delay.

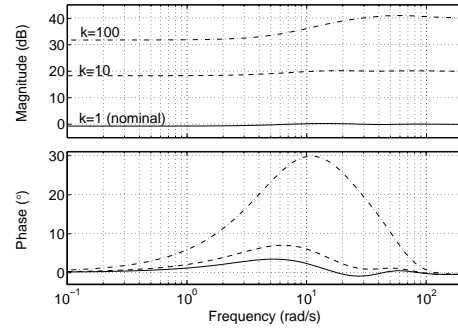


**Figure 6:** Bode plot of terminating impedance  $Z_x$  in nominal environment ( $k = 1$ ) and after changes in environmental stiffness ( $k = 10$ );( $k = 100$ ).

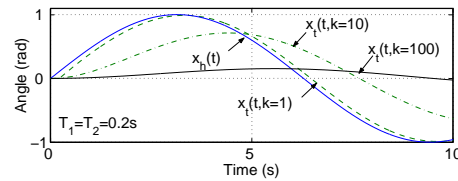


**Figure 7:** Position responses  $x_t(t)$  of teleoperator to HSI position  $x_h(t)$  input for different environmental stiffness coefficients  $k$ .

## 5 Experimental Results

The experimental setup consists of two identical single degree of freedom force feedback paddles connected to a PC; the original design of the paddles can be found in [11]. The basic configuration is shown in Fig. 8, where the teleoperator is connected to springs with the stiffness coefficient

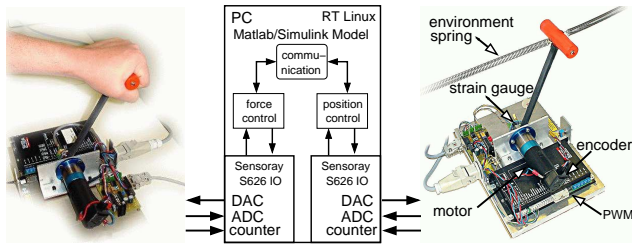


**Figure 8:** System hardware configuration.

$k = 162\text{N/m}$  and the damping coefficient  $b = 0.6\text{Ns/m}$ . The paddle DC motor torque is controlled by the PWM amplifier, which operates in current control with the reference given by a voltage from the D/A converter output of the I/O board. The force applied to the paddle lever, attached at the motor axis, is measured through the bending of the lever by a strain gauge bridge, that is attached at the bottom of the lever with the strain being amplified and converted by an A/D converter of the I/O board. The position of the lever, measured by an optic pulse incremental encoder on the motor axis is processed by a quadrature encoder on the I/O board. The control loops and the model of the communication channel are composed of MATLAB/SIMULINK block-sets; standalone realtime code for RT Linux is automatically generated from the SIMULINK model. All experiments were performed with a sample time  $T_A = 0.001\text{s}$ . In order to obtain a linear system a friction compensation and a gravity feedback linearization was applied. The compensation of unknown non-linearities was performed by model reference system synthesis with the reference system used in the simulations. The position and force responses of HSI and teleoperator of the optimized system in presence of time delay  $T_1 = T_2 = 0.2\text{s}$  in Fig. 9 show very good tracking performance, resulting in a transparent impression of the remote environment to the operator.

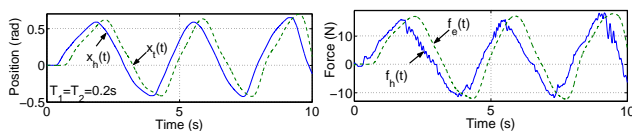


**Figure 9:** Time responses of position and force in spring environment with optimized filters.

## 6 Conclusions

A novel approach for position-force controlled telepresence systems has been proposed providing robust passivity and transparency by appropriately designed impedance matching filters. A frequency domain optimization method is used to obtain these filters with guaranteed passivity reserve. Numerical, simulation, and experimental results have shown that the proposed approach improves performance with respect to stability, tracking, and transparency. Future work is to generalize the presented methods for time-varying time delay and less known environments.

## Acknowledgment

This work has been partially supported by the “IBB-Zukunftsfond Berlin, Projekt Neue Generation leittechnischer Systeme (mobile und virtuelle Leittechnik)” co-financed by the EU with EFRE funds.

## References

- [1] N. Chopra, M. W. Spong, S. Hirche, and M. Buss, “Bilateral Teleoperation over Internet: the Time Varying Delay Problem,” in *Proceedings of the American Control Conference*, (Denver, CO), 2003, to appear.
- [2] M. Buss and G. Schmidt, “Control Problems in Multi-Modal Telepresence Systems,” in *Advances in Control: Highlights of the 5th European Control Conference ECC’99 in Karlsruhe, Germany* (P. Frank, ed.), pp. 65–101, Springer, 1999.
- [3] S. Salcudean, “Control for Teleoperation and Haptic Interfaces,” in *Lecture Notes in Control and Information Sciences 230: Control Problems in Robotics and Automation* (B. Siciliano and K. Valavanis, eds.), pp. 51–66, London: Springer, 1998.
- [4] R. Anderson and M. Spong, “Bilateral Control of Teleoperators with Time Delay,” *IEEE Transaction on Automatic Control*, vol. 34, pp. 494–501, 1989.
- [5] G. Niemeyer and J.-J. Slotine, “Stable Adaptive Teleoperation,” *IEEE Journal of Oceanic Engineering*, vol. 16, pp. 152–162, January 1991.
- [6] H. Baier, M. Buss, and G. Schmidt, “Stabilität und Modusumschaltung von Regelkreisen in Teleaktionssystemen,” *at—Automatisierungstechnik*, vol. 48, pp. 51–59, Februar 2000.
- [7] D. Lawrence, “Stability and Transparency in Bilateral Teleoperation,” *IEEE Transactions on Robotics and Automation*, vol. 9, pp. 624–637, October 1993.
- [8] B. Hannaford, “A design framework for teleoperators with kinesthetic feedback,” *IEEE Transactions on Robotics and Automation*, vol. 5, pp. 426–434, August 1989.
- [9] Y. Yokokohji and T. Yoshikawa, “Bilateral Control of Master-Slave Manipulators for Ideal Kinesthetic Coupling Formulation and Experiment,” *IEEE Transactions on Robotics and Automation*, vol. 10, pp. 605–619, October 1994.
- [10] G. Niemeyer and J. E. Slotine, “Using Wave Variables for System Analysis and Robot Control,” in *Proceedings of the IEEE International Conference on Robotics and Automation*, pp. 1619–1625, 1997.
- [11] H. Baier, M. Buss, F. Freyberger, J. Hoogen, P. Kammermeier, and G. Schmidt, “Distributed PC-Based Haptic, Visual and Acoustic Telepresence System—Experiments in Virtual and Remote Environments,” in *Proceedings of the IEEE Virtual Reality Conference VR’99*, (Houston, TX), pp. 118–125, 1999.